symmetry

MDPI

Review

The International Linear Collider Project—Its Physics and Status

Hitoshi Yamamoto [1,2,3]

[1] Graduate School of Science, Tohoku University, Sendai 980-0812, Japan; yhitoshi@epx.phys.tohoku.ac.jp or hitoshi.yamamoto@ific.uv.es; Tel.: +34-626-813-380
[2] Instituto de Física Corpuscular (IFIC), University of Valencia, 46980 Paterna, Spain
[3] Consejo Superior de Investigaciones Científicas (CSIC), 46003 Valencia, Spain

Abstract: The discovery of Higgs particle has ushered in a new era of particle physics. Even though the list of members of the standard theory of particle physics is now complete, the shortcomings of the theory became ever more acute. It is generally considered that the best solution to the problems is an electron–positron collider that can study Higgs particle with high precision and high sensitivity; namely, a Higgs factory. Among a few candidates for Higgs factory, the International Linear Collider (ILC) is currently the most advanced in its program. In this article, we review the physics and the project status of the ILC including its energy expandability.

Keywords: Higgs particle; elementary particles; standard theory; linear collider; dark matter; top quark

Citation: Yamamoto, H. The International Linear Collider Project—Its Physics and Status. *Symmetry* **2021**, *13*, 674. https://doi.org/10.3390/sym13040674

Academic Editor: Ayan Paul

Received: 23 March 2021
Accepted: 7 April 2021
Published: 13 April 2021

1. Introduction

In 2012, two experiments, ATLAS and CMS, operating at a proton–proton collider called the Large Hadron Collider (LHC), discovered the long-sought Higgs particle [1,2]. According to the standard theory of elementary particles (hereafter referred to as "the Standard Theory"), the field of Higgs particle filled the entire universe sometime after the Big Bang and gave masses to all the elementary particles currently known to have mass. Even now, the Higgs field is everywhere while we do not notice its existence. The Higgs particle is the only particle in the Standard Theory that has no electric charge nor spin, and as such it can "mimic" the vacuum of the universe. The Higgs particle is thus at the core of current particle physics.

The Higgs particle was the last to be discovered among the particles of the Standard Theory. Rather than completing the ultimate theory of particles, however, the discovery of the Higgs particle forces us to face serious shortcomings inherent in the Standard Theory. They include:

1. Dark matter is known to exist by cosmological observations and the cosmological theory, but there is no particle in the Standard Theory that can constitute the dark matter.
2. The Standard Theory cannot explain how the Higgs field came to fill the universe. In other words, it cannot explain the origin of the symmetry breaking.
3. The universe is dominated by matter over antimatter while the Big Bang with pair creations would indicate that the same amount of antimatter as matter should exist now. The Standard Theory cannot explain the matter–antimatter asymmetry observed today.
4. The measured mass of the Higgs particle receives contribution from fields of other particles clinging around it, and the mass correction predicted by the Standard Theory is many orders of magnitude greater than the measured Higgs mass itself. This is a highly unnatural situation suggesting that there exists a new and more fundamental theory that makes it natural.

These indicate that there are new physics beyond the Standard Theory. In fact, many new theories have been proposed to solve these problems and some of them could solve more than one shortcoming at the same time. For example, new theories such as those based on super-symmetry or extra dimensions attempt to solve the problem of Higgs mass, while in doing so they also provide candidates for dark matter.

A prominent feature of these new theories is that each theory contains a particle that is very much like the Higgs particle of the Standard Theory, but with slightly different properties, and the pattern of the deviations differ for each new theory. Thus, a high precision study of the Higgs particle should be able to elucidate which of these new theories is the true theory of nature, or if none satisfies the measurements, it could point to the true theory. In general, the higher the energy scale of new physics, the smaller the deviations; namely, the more precise are the measurements, the higher the energy scale that can be probed. A facility that is capable of such study may be an electron–positron collider at around 250 GeV, referred to as a 'Higgs factory', or a proton–proton collider at around 100 TeV. They are both capable of highly precise measurements needed. The cost and timescale of the latter, however puts it further in the future, and thus there exists at present a general agreement among the high energy physics community that an electron–positron collider is of the highest priority [3].

There are currently four proposals for an electron–positron Higgs factory: Two (International Linear Collider (ILC) and Compact Linear Collider (CLIC) [4]) are linear, where electrons and positrons are accelerated in opposite directions along a straight line and collide head-on at the center, and two (Future Circular Collider, ee version (FCCee) [5] and Circular Electron Positron Collider (CEPC) [6]) are circular, where electrons and positrons circulate in opposite directions in circular orbits and come to collide at one or more locations. The main merits for a linear collider are that beams can be polarized and that the collision energy can be upgraded (with due cost) later to much higher energies if physics demands. On the other hand, merits for a circular collider are that multiple collision points can be accommodated, luminosities at energies lower than 250 GeV such as on the Z pole are high, and that the same circular tunnel may be used for a proton–proton collider in the future.

While the capabilities of these machines as a Higgs factory are roughly equivalent, one of them—the International Linear Collider whose technical design report was completed in 2013 [7] and updated later [8–10]—is generally considered the most advanced as an international project.

In the following, we will review the technical status of the machine, the physics reach, and the project status of the ILC.

2. Machine

2.1. Overview of the Machine

At the ILC, an electron beam accelerated along a straight line to energy of 125 GeV collides head-on with a positron beam similarly accelerated in the opposite direction, resulting in collision energy of 250 GeV. Each beam consists of 5 trains per second (i.e., the "repetition rate" is 5 Hz) where one train is roughly 1 ms long consisting of 1312 bunches. One bunch contains 2×10^{10} particles and its size (rms) at the collision point is 7.7 nm high, 516 nm wide, and 300 µm long; namely, it is ribbon-like—very flat and long. A schematic drawing of the machine is shown in Figure 1.

Electrons are generated by hitting a photocathode with a strong laser and are captured and bunched. The electron bunch is then transported to the damping ring where the emittance is reduced to the desired level during the train gap of 200 ms. When all 1312 bunches are circulating in the damping ring with their emittance reduced, the bunches are extracted one by one to the far end of the linac to be accelerated to 125 GeV.

Before the electron bunch reaches the collision point, it goes through an undulator to generate an intense photon beam that hits a target to produce positrons which are then captured and bunched. The positron bunch is transported to the damping ring to reduce

its emittance (taking less than 200 ms), and then extracted to the opposite end of the linac to be accelerated to 125 GeV. It collides with an electron bunch of the next train. Just before collision, electron and positron bunches pass through a set of quadrupole magnets where the transverse sizes are reduced to the specified values.

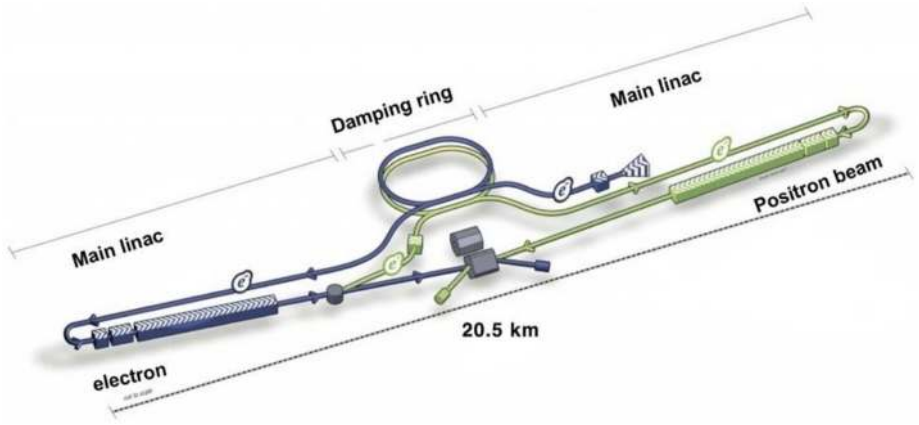

Figure 1. A schematic drawing of the International Linear Collider (ILC) (not to scale).

Surrounding the collision point is a state-of-the-art detector system designed to take full advantage of the clean environment of linear collider. It is envisioned that there will be two detectors in a push–pull mode—while one detector is taking data the other is undergoing upgrade or maintenance or simply standing by. Currently, two detector concept groups are actively engaged in R&Ds for the ILC: SiD and ILD [7].

With a polarized laser, electrons can have polarization of $\pm$80%. The photons generated by the undulator is naturally polarized, and the baseline design results in $\pm$30% polarization for positrons. As an option, the polarization of positron may be increased to $\pm$60% by using a longer undulator and limiting the phase space of created positrons. As a backup positron source, a conventional source is considered where electrons accelerated by a separate accelerator hit a target to produce positrons. This scheme allows enough positrons to be produced even when the electron energy is lower than about 125 GeV while the positrons produced this way are not polarized.

The luminosity may be upgraded by doubling the number of bunches per train or by doubling the repetition rate of the train. The luminosity is roughly doubled by each scheme and using both will result in increase of factor of bout four. The energy can be upgraded either by making the linac longer or by increasing the gradient of the acceleration. A collision energy of around 350 GeV is where the top quark pair creation threshold is located and around 500 GeV is where measurements of Higgs self-coupling and Higgs-top coupling become realistic. The basic machine parameters are summarized in Table 1.

Two key challenges of the ILC are to achieve high energy and to make the beams small. Below, we will briefly review current status of these issues followed by some details of upgrades.

2.2. Accelerating Beams

The ILC is based on a superconducting accelerator technology, and the development of high-gradient RF cavity plays a central role. At the linac, beams are accelerated in 1.3 GHz 9-cell superconducting cavities made of high-purity niobium immersed in a liquid helium bath at 2K (Figure 2). Since the cost of linac for a given final beam energy is roughly inversely proportional to the accelerating gradient, there is a strong interest in achieving as high gradient as possible. The ILC specification of the accelerating gradient is 35 MV/m $\pm$20% for initial testing ("vertical test") corresponding to approximately 31.5 MV/m when in use. It translates to ~4 km of acceleration, or ~4000 cavities, to achieve the acceleration to 125 GeV.

Table 1. The ILC machine parameters for 250 GeV Higgs factory and energy upgrades [9]. Values for TDR 250 GeV [7] are also shown as reference. The 'L Upgrade' column is the luminosity upgrade by doubling the number of bunches. For 500 GeV, the luminosity upgrade version is also shown. Once the energy is upgraded to 500 GeV (after the number of bunch is doubled), the machine can be operated at 250 GeV with repetition rate of 10 Hz, which results in a luminosity of $5.4 \times 10^{34}/\mathrm{cm}^2\mathrm{s}$.

Quantity	Unit	Baseline	L Upgrade	TDR	Energy Upgrades	
Centre of mass energy	GeV	250	250	250	500	1000
Luminosity	$10^{34}/\mathrm{cm}^2\mathrm{s}$	1.35	2.7	0.82	1.8/3.6	4.9
Polarization for e-(e+)	%	80 (30)	80 (30)	80 (30)	80 (30)	80(20)
Repetition frequency	Hz	5	5	5	5	4
Bunches per pulse	1	1312	2625	1312	1312/2625	2450
Bunch population	10^{10}	2	2	2	2	1.74
Linac bunch interval	ns	554	366	554	554/366	366
Beam pulse duration	μs	727	961	727	727/961	897
Norm. hor. emitt. at IP	nm	5	5	10	10	10
Norm. vert. emitt. at IP	nm	35	35	35	35	30
Hor. beam size at IP	nm	516	516	729	474	335
Vert. beam size at IP	nm	7.7	7.7	7.7	5.9	2.7
Site AC power	MW	129		122	163/204	300
Site length	km	20.5	20.5	31	31	40

Figure 2. A 1.3 GHz 9-cell superconducting cavities for the ILC. The length is 1.25 m.

Cavities similar to the ILC cavities are used for the European X-ray Free Electron Laser facility (E-XFEL) for which 832 9-cell cavities were produced and tested [11]. Even though the gradient specification of ~26 MV/m for E-XFEL is lower than for the ILC, this represents a highly reliable sample for estimating the yield and cost of cavity production for the ILC. Figure 3 shows the distribution of the maximum gradient of cavities produced for the E-XFEL by two vendors [11]. Vendor RI employs a production process that closely follows the ILC procedures and achieves a better performance. The yield is ~95% yield for the ILC specification of >35 MV/m−20% (=28 MV/m). Overall, the E-XFEL experience indicates that the ILC goal for cavity production can be met. In addition, the cost estimate of the ILC cavity production is firmly based on the experience of the E-XFEL.

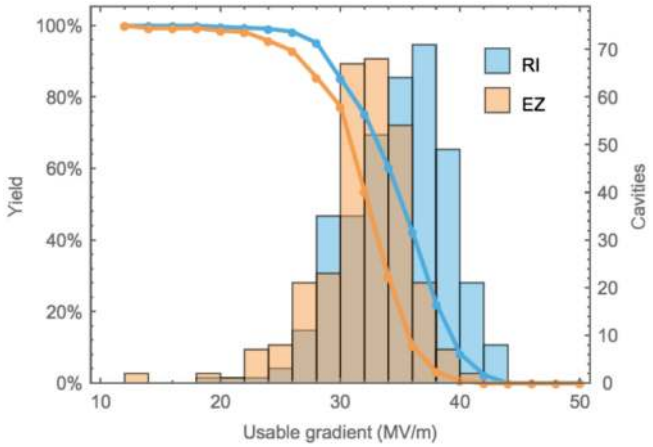

Figure 3. Maximum gradient and yield of 'as received' cavities produced for the European X-ray Free Electron Laser (E-XFEL) by two vendors [11]. Vendor RI employs a production process that closely follows the ILC specification.

Eight or nine 9-cell cavities are assembled into one cryomodule that provides support and cooling. Since cavities and cryomodule parts are manufactured in different parts of the world, a question arises if they can be successfully assembled without degrading the performance. For this purpose, "plug compatibility" designs are adopted, where the designs of connection points are rigorously defined. To test the idea in practice, a so-called "S1-Global" project (Figure 4) was performed in which parts produced all over the world were brought to the KEK laboratory in Japan to be assembled together. The result was satisfactory.

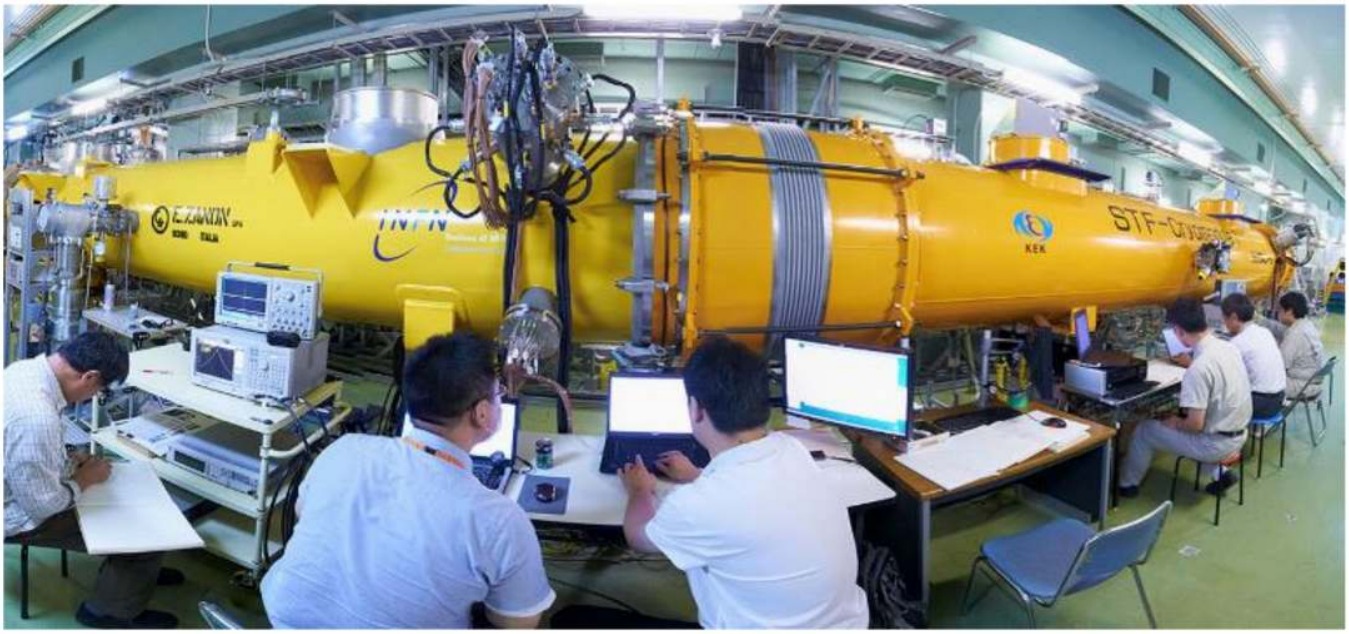

Figure 4. The "S1-Global" project in which parts manufactured at different locations all over the world are assembled together with "plug-compatible" designs.

2.3. Making the Beam Smaller

In order to make the beam smaller, the emittance of the beam has to be reduced. Emittance is zero when particles in the beam focus to a single point or when they are parallel in which case they can be focused to a point with a perfect lens. The emittance is reduced by the damping ring where particles are encouraged to emit photons by bending magnets or by wiggler magnets. The lost energy by the photon emission is recovered by acceleration in the direction of design orbit. By repeating the process, all particles tend to move in the design direction, thus reducing the emittance.

The test facilities ATF and ATF2 are located at the KEK accelerator laboratory. ATF is a damping ring test facility to produce super-low emittance. There, the ILC goal was achieved for both vertical and horizontal emittances. At ATF2, the beam is stabilized and focused. Figure 5 shows the achieved vertical beam size as a function of time. A vertical beam size of 41 nm has been achieved while the ILC goal is 37 nm; namely, the goal is more or less achieved. Note that when a beam is accelerated, the emittance becomes smaller since they tend to become more parallel, and thus the beam size is reduced. The beam size of 37 nm at the ATF beam energy of 1.3 GeV corresponds to 5.9 nm at 250 GeV.

Figure 5. The achieved vertical beam size at ATF2 facility [9]. The latest value of 41 nm is within 10% of the goal of 37 nm.

2.4. Staging and Upgrades

At the time of the TDR, the baseline collision energy was 500 GeV, and the TDR machine parameters for 250 GeV collision were simply scaled from the 500 GeV design assuming the same horizontal beam size. The horizontal beam size, however, is limited by the beam background, which is less severe at 250 GeV, allowing a smaller horizontal beam size. The new baseline design for 250 GeV collision thus uses a horizontal emittance that is $\frac{1}{2}$ of the TDR value, resulting in a horizontal beam size that is smaller by $1/\sqrt{2}$. This increases the geometric luminosity by $\sqrt{2}$, and when the pinching effect where the colliding bunches focus each other is included, the overall increase becomes a factor of 1.65.

As mentioned in the introduction, the luminosity can be doubled by simply doubling the number of bunches per train. This can be done for 250 GeV as well as for 500 GeV and requires 50% more klystrons and modulators to drive the cavities. Additionally, a second damping ring for positron may be needed. A detailed cost estimate for such an upgrade was done for the 500 GeV case, and the cost increase of the overall machine was 6% including the second damping ring for positron. A similar estimate for the 250 GeV case has not been done, but the relative cost increase is expected to be similar to the 500 GeV case. The AC power for the 500 GeV case is estimated to increase from 163 MW to 204 MW by doubling the number of bunches. Again, a similar estimate for the 250 GeV case has not been done, but it is safe to assume that the increase of AC power is less than 25%.

The luminosity at 250 GeV can also be doubled by doubling the train repetition rate from 5 Hz to 10 Hz. This requires a cryogenic system equivalent to that of the 500 GeV machine. The cost and AC power of such machine would then be similar to those of the 500 GeV machine. Indeed, it may make sense to first double the number of bunches starting from the 250 GeV baseline with 5 Hz repetition rate, then upgrade the energy to 500 GeV with the same number of bunches and the same repetition rate, and then lower the energy back to 250 GeV with 10 Hz repetition rate. This would result in a luminosity four times greater than that of the baseline 250 GeV machine.

As stated in introduction, the collision energy of the machine can be increased in two ways: One is simply by making the linac longer, and the other is by increasing the gradient of the acceleration. The design of the beam delivery system leading to the interaction point is such that minor modification can accommodate collisions of up to 1 TeV. When the length of the linac increases, the turn-around at the end of linac needs to be relocated. The Kitakami candidate site can accommodate at least up to 50 km while the length of the machine is 20.5 km for 250 GeV collision. The achievable gradient at the time of energy upgrade is difficult to predict. If we assume the same gradient of 31.5 MV then the length of the 500 GeV machine would be 31 km.

Figure 6 shows the collision energies and luminosities of the four proposed electron-positron Higgs factories based on information submitted to the 2020 European Strategy of Particle Physics Update [3]. The luminosities are for single interaction point. While the two circular machines (FCCee and CEPC) have two interaction points each in their CDRs, the

effective increase of luminosity due to polarization is not included for linear colliders (ILC and CLIC).

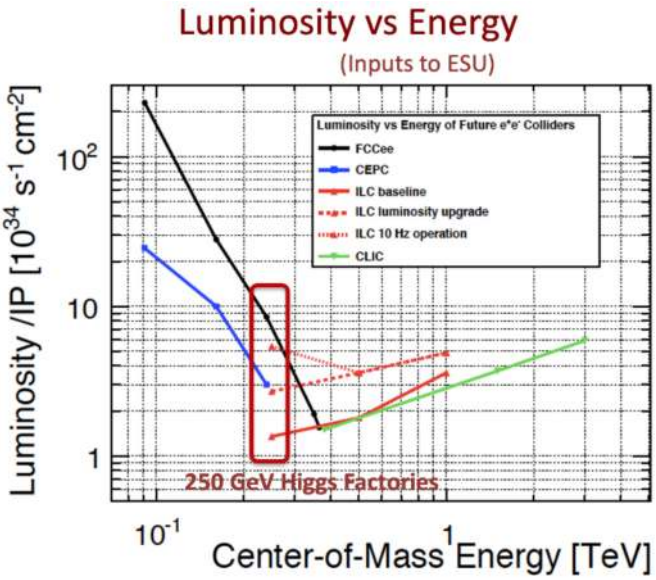

Figure 6. The luminosity vs. center-of-mass energy for the four candidates for electron-positron Higgs factory. The luminosity is for single interaction point while the effect of polarization is not included ([9], and references therein).

3. Physics

In the history of particle physics, proton machines and lepton machines played complementary roles. Particles such as the Z vector boson were discovered at a proton machine (SPS) and then studied in detail at lepton machines (SLC and LEP). History may repeat itself for the new era of particle physics opened by the discovery of the Higgs particle.

Advantages of an electron–positron linear collider are:

1. Events are clean since it is a collision of elementary particles. For example, most of the particles observed in a given Higgs event, or often all the particles, originate from the decay of the Higgs particle itself without many extra particles.
2. One knows the 4-momentum of the initial state of the electron–positron collision. This can be used, for example, to reconstruct an invisible particle by detecting particles recoiling against that particle and reconstructing the recoil mass.
3. The beam can be polarized. This adds a new dimension to the measurement, allowing us to probe those phenomena not accessible otherwise. In addition, in some important cases, one can turn off dominant backgrounds created by left-handed electron interactions by using a right-handed electron beam.

As stated in introduction, precision Higgs measurements are the most important physics topic of the ILC; thus, the name "ILC Higgs factory". On the other hand, high precision translates to high sensitivity that could reveal new particles that may be missed at the LHC if the particle is within the energy reach of the ILC. The upgraded LHC will have impressive capabilities to find new particles. One should note, however, that even though some 20,000 Higgs particles were generated at the Tevatron (a proton–antiproton collider), a clear signal of the Higgs particle had to wait for the LHC. At a linear collider, only tens of generated Higgs would have been sufficient to have established a Higgs discovery.

Another important physics is related to the top quark that is accessible when the collision energy is upgraded to above 350 GeV. The top quark is the heaviest particle in the Standard Theory, and there are models beyond the Standard Theory in which properties of the top quark deviate from those of the Standard Theory.

3.1. Higgs Physics

At the ILC Higgs factory, the main channel to produce Higgs particles is the so-called Higgsstrahlung process $e^+e^- \to HZ$ as shown in Figure 7a. The cross sections of this process as well as other processes to produce Higgs particles—the vector-fusion processes $e^+e^- \to H\nu\bar{\nu}$, He^+e^-—are shown in Figure 7a. The cross section of the Higgsstrahlung process peaks around collision energy of 250 GeV.

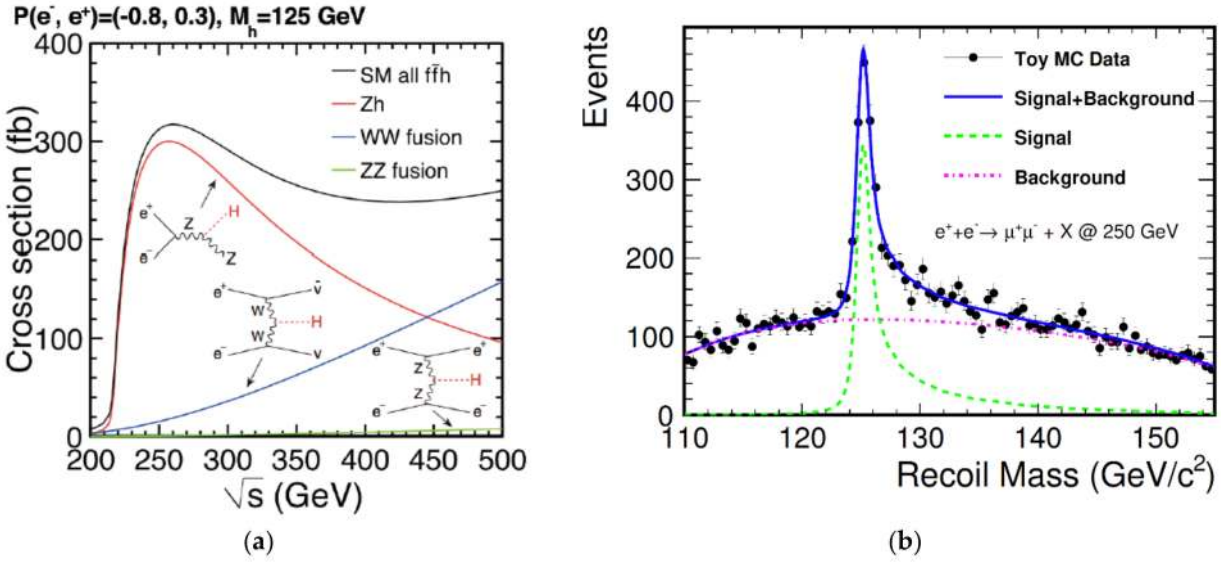

Figure 7. (**a**) The processes to produce Higgs particles at the ILC Higgs factory [4]. (**b**) Reconstruction of Higgs particle with the recoil mass technique at collision energy of 250 GeV [12].

The Higgsstrahlung process offers a technique to reconstruct the Higgs particle without detecting its decay. Namely, by detecting the Z particle and calculating the invariant mass of the system recoiling against it, one can reconstruct the Higgs particle without actually detecting its decay products. A recoil mass distribution for the ILC running at 250 GeV is shown in Figure 7b [12]. This allows an absolute determination of the ZH coupling. It also enables the measurement of the branching fraction of Higgs particle decaying to an invisible final state with accuracy below 1% [13]. Through the recoil mass technique, the Higgs mass can be determined to better than 30 MeV [13].

3.1.1. Higgs Coupling Measurements

Often-used approaches for analyzing Higgs couplings are the so-called "κ framework" and the effective field theory approach. In the κ framework, one assumes the same interaction forms as in the Standard Theory and simply varies the size of a coupling constant to fit the observed partial decay rate:

$$\frac{\Gamma(H \to X)}{\Gamma(H \to X)_{SM}} = \kappa^2$$

where "SM" indicates the partial decay rate expected by the Standard Theory. In the effective field theory approach, one assumes the SU(2) × U(1) gauge symmetry of the Standard Theory and take all relevant terms up to dimension-6 to perform a global fit for the coupling constants. In this effective field theory approach, radiative corrections are in principle calculable and the effect of polarization is taken into account in a natural way. On the other hand, the effect of polarization is explicitly ignored in the κ framework. We will use the effective field theory approach in this article.

In general, the Higgs total decay rate is required to convert measured absolute branching ratios to coupling constants. The total decay rate can be obtained from the Higgs

branching ratio to WW together with the partial decay rate to WW calculated from the HW coupling constant measured by the WW fusion production rate. It could also be obtained from the branching ratio to ZZ combined with the partial decay rate to ZZ calculated from the HZ coupling constant measured by the $e^+e^- \to HZ$ production rate. However, the Higgs to ZZ branching ratio is quite small, and the W fusion production rate at 250 GeV is also small, as can be seen in Figure 7a. As a result, neither method is not ideal. In the effective field theory approach, the SU(2) × U(1) gauge symmetry introduces a certain relation between the HZ coupling and the HW coupling, making a high-precision Higgs coupling analysis possible at 250 GeV.

3.1.2. Projected Precisions for Higgs Couplings

Precisions expected for Higgs couplings are shown in Table 2. The second column corresponds to the case where 2 ab^{-1} of data taken at 250 GeV ILC is added to the results from the upgraded LHC [14], and the third column is when 4 ab^{-1} of data taken at 500 GeV ILC is included in addition. Expected result on $e^+e^- \to WW$ at the ILC as well as currently available precision electroweak results are also included. In order to make the analysis as model-independent as possible, Higgs decays to exotic states and invisible state are included in the fit. The global fit in the effective field theory framework gives the coupling constants of the interaction terms and their errors, while a given Higgs coupling in the table in general corresponds to more than one terms. The quoted relative uncertainties are one half of those of corresponding partial decay rates calculated from the result of the global fit.

Table 2. Precisions expected for Higgs couplings for 2 ab^{-1} of data taken at 250 GeV and for 4 ab^{-1} of data taken at 500 GeV in addition to the 250 GeV data [9]. Results from the upgraded LHC are also included.

Unit: %	250 GeV, 2 ab^{-1}	500 GeV, 4 ab^{-1}
HZZ	0.56 (0.47)	0.38 (0.33)
HWW	0.55 (0.47)	0.37 (0.33)
Hbb	1.0 (0.81)	0.60 (0.49)
$H\tau\tau$	1.2 (0.98)	0.77 (0.68)
Hgg	1.6 (1.2)	0.96 (0.75)
Hcc	1.8 (1.4)	1.2 (0.9)
$H\gamma\gamma$	1.1 (1.1)	1.0 (1.0)
$H\gamma Z$	7.5 (7.0)	4.0 (3.5)
$H\mu\mu$	4.0 (4.0)	3.8 (3.8)
Htt	-	6.3 (4.5)
HHH	-	27 (20)
G_{tot}	2.4 (1.9)	1.6 (1.3)
G_{inv}	0.36 (0.36)	0.32 (0.32)

The numbers in parentheses are for an optimistic projection for the ILC analysis where plausible improvements in detection efficiencies and systematic errors are assumed as well as an inclusion of the measurement of the left-right asymmetry parameter A_l at 250 GeV ILC using radiative return events (for the detail of the assumptions made, refer to [9]).

The improvements obtainable by adding ILC data to the upgraded LHC data is shown in Figure 8. All cases assume that the Higgs decay final states are limited to those of the Standard Theory and that there are no anomalous forms of HZ and HW couplings. Actually, these assumptions are not necessary for the ILC which, in fact, is an important merit for the ILC. They are made here for the sake of comparison. First, we see that there is no data of Hc for LHC where the charm tagging is challenging. For the ILC, the excellent vertex identification capability makes it possible to separate out charm quarks. The improvements for HZ and HW are impressive due to the measurement of the Higgs production rate. For the Hb coupling, the b-tagging capability of the ILC plays an important role. On the other

hand, improvements for $H\mu$, $H\gamma$, and Ht are not significant. In particular, 500 GeV ILC is required for measurements of these coupling constants.

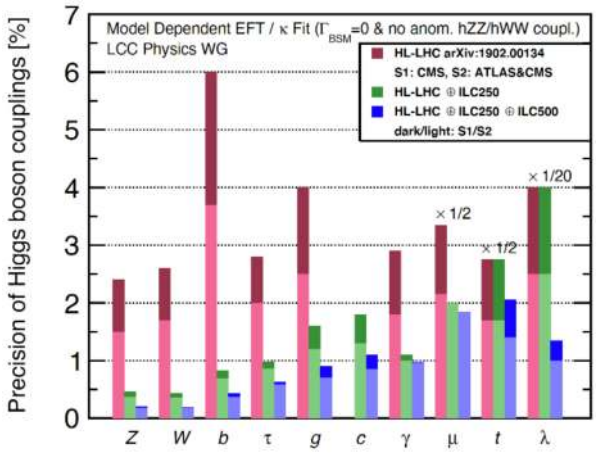

Figure 8. Improvements by adding ILC data to the upgraded LHC data [9]. The all analyses assume that there are no Higgs decay final states other than those of the Standard Theory and that the forms of HZ and HW couplings are the same as those of the Standard Theory. For each bar, the light (dark) color corresponds to an optimistic (conservative) projection.

The Higgs self-coupling parameter λ comes from the term of the Higgs potential that is cube of the Higgs field measured as a deviation from the value of the vacuum. This indicates that the Higgs potential is not symmetric with respect to the vacuum. Since the original Higgs potential is expected to be symmetric with respect to the original vacuum, the Higgs self-coupling indicates that the vacuum has shifted from the original point to a local minimum. Thus, the Higgs self-coupling can be said to be a smoking gun of the symmetry breaking. In general, there can also be a quadratic term, but it is far more difficult to measure and, in this article, Higgs self-coupling is understood to refer to the 3-point Higgs self-coupling.

The Standard theory predicts a continuous phase transition for the symmetry breaking and leads to a specific value for the Higgs self-coupling. On the other hand, new theories with first-order phase transition tends to have Higgs self-couplings that are different from that of the Standard Theory [15–17]. Thus, the value of the Higgs self-coupling gives information on the nature of the symmetry breaking that caused the Higgs field to 'freeze' at a certain value. The 3-point self-coupling can change a single Higgs particle to two Higgs particles. Thus, the modes to search are the single Higgs Production modes where one Higgs particle replaced with two Higgs particles. At the 500 GeV ILC, the signal mode is $e^+e^- \to HHZ$, and the current state of the art is that the Higgs self-coupling can be measured to 27% with the full dataset [18]. At 1 TeV, $e^+e^- \to HH\nu\bar{\nu}$ mode is detected to give the Higgs self-coupling to 16% with 2 ab^{-1} of data [18]. The measurement of the Higgs self-coupling is challenging at any facility.

3.1.3. Impact of Polarizations

In Figure 9, relative precisions obtainable by the data with and without polarizations are shown for Higgs couplings to various particles as well as for the partial decay rate to invisible final state and the total Higgs decay rate. They all correspond to the cases where the results of the ILC are combined with those of upgraded LHC (HL-LHC). The dark green shows the precisions obtainable by 2 ab^{-1} of data at the ILC250 (Higgs factory) with polarizations and the dark red by 5 ab^{-1} of ILC250 data without polarizations. Relative merits with polarizations depend on modes and simple conversion to a gain factor of effective luminosity is not possible. One can see, however, that 2 ab^{-1} of data with polarizations is roughly equivalent to 5 ab^{-1} of data without polarizations.

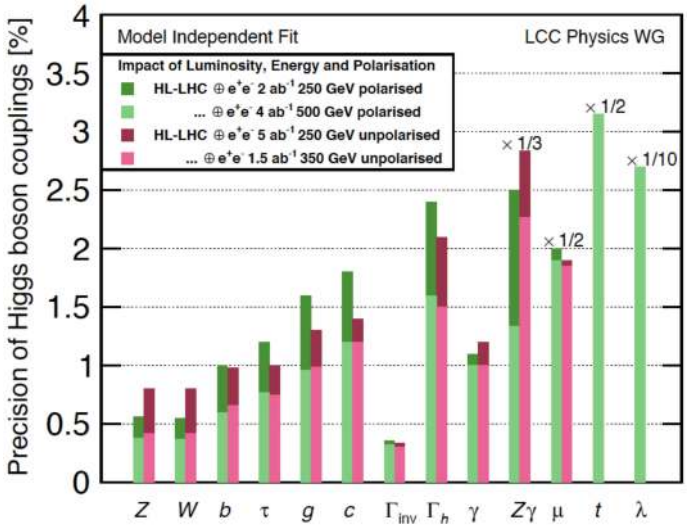

Figure 9. Relative precisions obtainable by the data with and without polarizations [9]. The results of the ILC are combined with those of upgraded LHC (HL-LHC). The polarizations are assumed to be ±80% for electrons and ±30% for positrons, and the data is divided to (−+, +−, ++, −−) = (45%, 45%, 5%, 5%).

3.1.4. Separation of Models

These precision measurements make it possible to distinguish different new physics scenarios through the pattern of deviation from the Standard Theory. Figure 10 shows the separation power of the ILC Higgs factory for 9 models that are unlikely to be rejected by the upgraded LHC. The number in each grid is the number of standard deviations between the two models represented by the grid. In most cases, the models can be distinguished with significance of several standard deviations. Thus, it can be said that the ILC Higgs factory can more or less pinpoint the correct theory or if the true theory is not in the list of proposed theories, it can tell what kind of theory is the true theory.

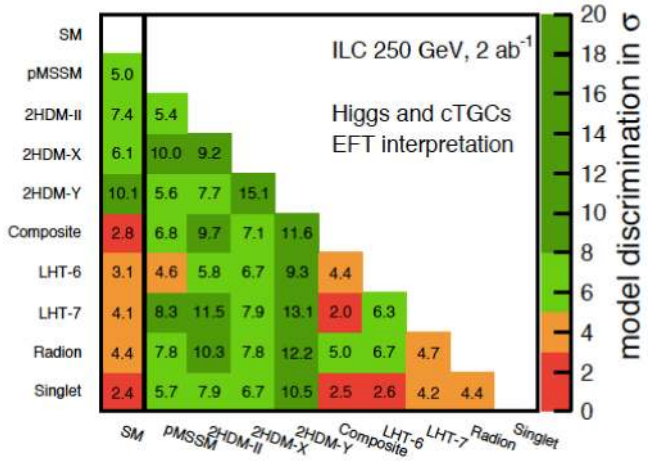

Figure 10. Separation powers of the ILC Higgs factory for 9 new theoretical models beyond the Standard Theory that are considered unlikely to be rejected by the upgraded LHC [19].

3.2. Search for New Particles

At the ILC, new particles may be pair-created where the pair may be the same particle type or they may be different. Often, the pair-created particle would decay to an invisible particle emitting a soft ordinary particle such as W, τ, or μ. When the pair are the same type, the maximum and minimum end points of the energy distribution of the ordinary particle simultaneously gives the masses of the pair-created new particle and that of the invisible particle. In some of well-motivated and natural models for new physics, the mass

difference between the new particles is small (about 20 GeV or less). At hadron machines such as LHC, these signals are difficult to detect since the ordinary particle is soft and identifying them would be like searching a needle in a haystack, while a linear collider can detect such signals in most cases. In general, the discovery potential at the ILC extends essentially up to the beam energy for nearly all models and their parameter spaces.

Figure 11 shows an example for the case where the new particle is smuon $\tilde{\mu}$ (the super partner of muon in supersymmetric models) decaying to a dark matter candidate and a muon. The dark matter candidate escapes without interaction with the detector, and the signature of event is a pair of soft muons. The discovery potential is seen to extend close to the beam energy.

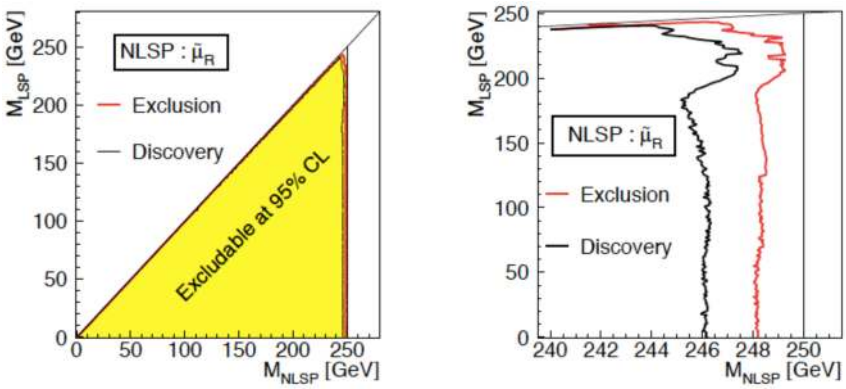

Figure 11. An example for pair creation of new particle that decays to the dark matter candidate and a muon: $e^+e^- \to \tilde{\mu}^+\tilde{\mu}^-$, $\tilde{\mu} \to \chi\mu$ [9]. The regions for 5σ discovery and 95% exclusion are shown. The analysis corresponds to 500 fb^{-1} of data taken at collision energy of 500 GeV. The signature for 250 GeV collision energy is essentially the same.

Dark matter candidates are usually conpletely invisible to the detector. Even in such senarios, the signal can be detected using the recoil mass of a detected initial-state photon in $e^+e^- \to \chi\chi\gamma$ where χ is the invisible particle [19,20], where the energy and angular distributions of the detected photon give information on the invisible particle.

3.3. Top Quark

At the ILC, the top quark can be studied either around the threshold of the pair creation (~350 GeV) or well above the threshold.

At the threshold, the production cross section as a function of collision energy gives information on key top parameters; in particular, the mass and the total decay rate as shown in Figure 12. The top mass measured by the shape of the production cross section is closely related to the so-called $\overline{ms}$ mass that is relevant to various theoretical applications. The statistical errors on the top mass and its total decay rate are estimated to be 16 MeV and 21 MeV [21,22], respectively, for a 200 fb^{-1} of data taken around the threshold. This top mass can be translated to the $\overline{ms}$ mass with a systematic error of ~10 MeV [23].

At well above the threshold, the angular distribution of the pair produced top quark with respect to the incoming electron beam is sensitive to the right-handed and left-handed top coupling to the intermediate Z particle. This is particularly true with the capability of a linear collider to polarize the incoming beams. Figure 13 shows the deviation from the Standard theory for the right-handed and left-handed couplings for a variety of models beyond the Standard Theory [24]. One can see that many new physics theories can be distinguished with the precision of the ILC.

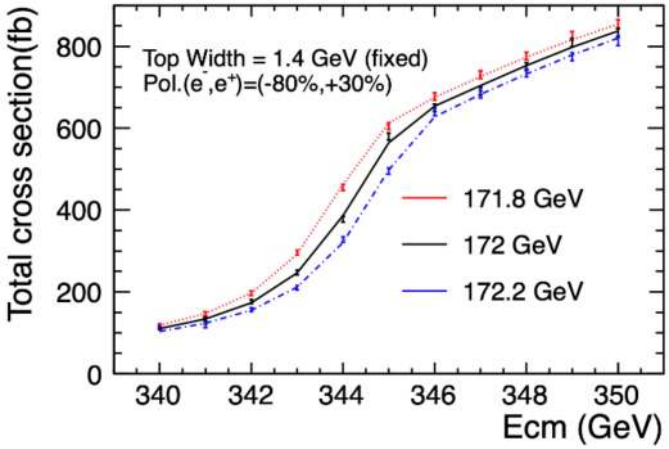

Figure 12. At the threshold of top pair production, the top mass and decay rate can be measured with high precision [22].

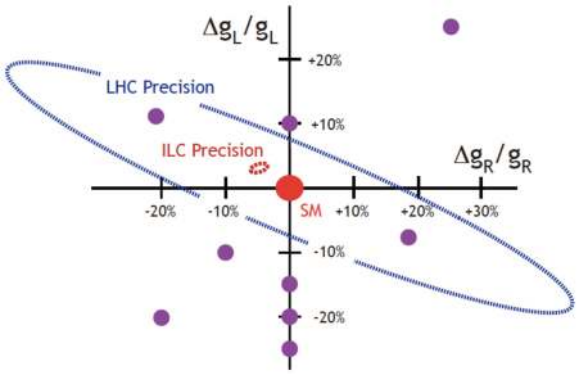

Figure 13. The right–handed and left–handed top coupling to the Z are shown for the Standard Theory and other new theories. The ILC precision is shown as the dotted red oval near the center [24].

4. Project Status

The 4-volume ILC technical design report [4] was completed in June 2013. This was a culmination of the international efforts managed by the Global Design Effort (GDE) and the research directorate (RD). The activity of GDE and RD were passed on to a new organization—the Linear Collider Collaboration (LCC) led by its director Lyn Evans. The main goal of the LCC was to realize the ILC. The LCC was supervised by the Linear Collider Board, which in turn was under the International Committee for Future Accelerators (ICFA).

There have been strong international supports for the ILC. Recent ones include the statement of the 2020 European Strategy of Particle Physics Update [3]: "The timely realization of the electron-positron International Linear Collider (ILC) in Japan would be compatible with this strategy and, in that case, the European particle physics community would wish to collaborate." It is also noteworthy that the US State Department issued a supporting statement at a conference on linear collider [25], saying "the U.S. Department of State has done our initial due diligence, and we are ready to assist our partner agencies in moving forward with the next major particle physics facility in Japan—the International Linear Collider, also known as the ILC."

Based on the discussions at the LCB meeting held in Palo Alto, California on 22 February 2020, ICFA decided in August 2020 to advance the ILC project to the next phase by establishing the International Development Team (IDT) whose mandate is to make preparations toward the ILC Pre-Laboratory (Pre-Lab). The IDT would complete its work by the end of 2021.

The Pre-Lab is to solve remaining technical issues of the accelerator, design the organization and functions of the ILC laboratory, and launch the ILC laboratory. The Pre-Lab is to last for 4 years followed by 10 years of construction under the ILC laboratory.

Status in Japan

In order to deal with this new development, the Japan High Energy Physics Committee that represents the Japanese high energy physics community established the ILC Steering Panel (http://jahep-ilc.org/en/, accessed on 11 April 2021) in October 2020. The charge for the panel is to develop and execute coherent promotion strategies under close coordination with IDT and KEK. It cooperates with other scientific communities, governmental authorities, legislators, corporate leaders, regional governments, media, as well as international communities and authorities.

At the political level in Japan, a non-partisan group, the Federation of Diet Members for the ILC ("Federation") was formed in 2006. It consists of over 100 members out of a total of 710 Diet Members. Federation members meet frequently to discuss the strategies to realize the ILC and have interacted closely with counterparts of possible international partners. They have visited the United States (2013~) and Europe (2016~) numerous times in order to discuss the ILC.

Within the ruling party, the Liaison Committee for Realizing the ILC ("Committee") was formed with a large fraction of the key members of the party in 2018 aiming to realize the ILC by elevating the project as a national priority across policies. In February 2019, the Federation and the Committee jointly approved a resolution urging the Japanese government to host the ILC as a cross-policy national project.

On 5 June 2020, the National Diet of Japan passed a bill to extend the term of the Reconstruction Agency whose mandate is to manage the reconstruction after the Great East Japan Earthquake. One of its supplementary resolutions mentioned the ILC: "Since the Tohoku area is the world's candidate site for the International Linear Collider project, its implementation will contribute, alongside the Fukushima Innovation Coast Framework, to the creation of a "New Tohoku" by becoming a breeding ground for scientific innovation. Therefore, the discussions need to be pushed forward in close coordination with the relevant organizations toward realizing the ILC in Japan" (unofficial translation).

The Advanced Accelerator Association Promoting Science and Technology (AAA, http://aaa-sentan.org/en/, accessed on 11 April 2021) is the industry–academia collaboration that supports the ILC. It is chaired by a former CEO of Mitsubishi Heavy Industries and consists of over 100 companies and over 40 academic institutes. It supports the delegation of the Federation to the US and Europe by providing financial and logistical support while engaging in technological R&Ds including the clean technologies for ILC ("Green ILC").

Local efforts in the Tohoku Region where the candidate site of the ILC is located are coordinated by the Tohoku ILC Promotion Council (https://en.tohoku-ilc.jp/, accessed on 11 April 2021) and its preparation office—the Tohoku ILC Project Development Center (https://tipdc.org/en, accessed on 11 April 2021). They address regional issues such as geological and hydrological survey, infrastructure development, and environmental assessment. The Tohoku ILC Promotion Council consists of academia (10), industries and business (203), and local governments (18), and its annual meetings are attended by Prefectural Governors (2) and Mayors (6). Some of the local governments have their own organizations to promote the ILC.

5. Conclusions

The ILC has been designed to play a leading role in the new era of particle physics ushered in by the discovery of the Higgs particle. Thanks to the cleanliness of its events as well as the capability to control the initial state of the collision, the ILC has sensitivities to the properties of the Higgs particle iggsHiggs that greatly upgrade the ultimate LHC precisions. Additionally, for new particle searches, the ILC provides impressive capabilities to uncover new physics that may be difficult to find at the LHC. The international and

domestic supports are strong and the project is now moving toward the PreLab that is to prepare for the ILC laboratory to start construction.

Funding: No external funding was received for this review article.

Institutional Review Board Statement: Not applicable.

Informed Consent Statement: Not applicable.

Acknowledgments: I would like to thank the *Symmetry* magazine who suggested that I write this article, and patiently waited for my late completion. I also would like to thank all those who contributed to the enormous amount of efforts related to this subject.

Conflicts of Interest: The author declares no conflict of interest.

References

1. ATLAS Collaboration. Observation of a new particle in the search for the Standard theory Higgs boson with the ATLAS detector at the LHC. *Phys. Lett. B.* **2012**, *716*, 1. [CrossRef]
2. CMS Collaboration. Observation of a new boson at a mass of 125 GeV with the CMS experiment at the LHC. *Phys. Lett. B.* **2012**, *716*, 30. [CrossRef]
3. The European Strategy Group. 2020 Update of the European Strategy for Particle Physics. Available online: https://home.cern/sites/home.web.cern.ch/files/2020-06/2020%20Update%20European%20Strategy.pdf (accessed on 11 April 2021).
4. CLIC (Compact Linear Collider). Available online: https://home.cern/science/accelerators/compact-linear-collider (accessed on 11 April 2021).
5. FCCee (Future Circular Collider, ee Version). Available online: https://home.cern/science/accelerators/future-circular-collider (accessed on 11 April 2021).
6. CEPC (Circular Electron Positron Collider). Available online: http://cepc.ihep.ac.cn (accessed on 11 April 2021).
7. Linear Collider Collaboration. The International Linear Collider Technical Design Report. Vol 1, Executive Summary. *arXiv* **2013**, arXiv:1306.6327.
8. Evans, L.; Michizono, S. The International Linear Collider Machine Staging Report 2017. *arXiv* **2017**, arXiv:1711.00568.
9. Linear Collider Collaboration. The International Linear Collider: A Global Project. *arXiv* **2017**, arXiv:1903.01629.
10. Harrison, M.; Ross, M.; Walker, N. Snowmass on the Mississippi. In Proceedings of the 2013 Community Summer Study on the Future of U.S. Particle Physics (CSS2013), Minneapolis, MN, USA, 29 July–6 August 2013.
11. Reschke, D.; Gubarev, V.; Schaffran, J.; Steder, L.; Walker, N.; Wenskat, M.; Monaco, L. Performance in the vertical test of the 832 nine-cell 1.3 GHz cavities for the European X-ray Free Electron Laser. *Phys. Rev. Accel. Beams* **2017**, *20*, 042004. [CrossRef]
12. Yan, J.; Watanuki, S.; Fujii, K.; Ishikawa, A.; Jeans, D.; Strube, J.; Tian, J.; Yamamoto, H. Measurement of the Higgs boson mass and $e^+e^-\to ZH$ cross section using $Z\to\mu^+\mu^-$ and $Z\to e^+e^-$ at the ILC. *Phys. Rev. D* **2016**, *94*, 113002. [CrossRef]
13. The Physics Working Group of the LCC. Physics case for the international linear collider. *arXiv* **2015**, arXiv:1506.05992.
14. Cepeda, M.; Gori, S.; Ilten, P.; Kado, M.; Riva, F.; Abdul Khalek, R.; Aboubrahim, A.; Alimena, J.; Alioli, S.; Alves, A.; et al. Physics of the HL-LHC Working Group. *arXiv* **2019**, arXiv:1902.00134.
15. Grojean, C.; Servant, G.; Wells, J.D. First-Order Electroweak Phase Transition in the Standard theory with a Low Cutoff. *Phys. Rev. D* **2005**, *71*, 036001. [CrossRef]
16. Noble, A.; Perelstein, M. Higgs Self-Coupling as a Probe of Electroweak Phase Transition. *Phys. Rev. D* **2008**, *78*, 063518. [CrossRef]
17. Aoki, M.; Kanemura, S.; Seto, O. Neutrino mass, Dark Matter and Baryon Asymmetry via TeV-Scale Physics without Fine-Tuning. *Phys. Rev. Lett.* **2009**, *102*, 051805. [CrossRef] [PubMed]
18. Tian, J. Study of Higgs Self-Coupling at the ILC Based on the Full Detector Simulation at $\sqrt{s}$ = 500 GeV and $\sqrt{s}$ = 1 TeV, LC-REP-2013-003. Available online: http://www-flc.desy.de/lcnotes/notes/LC-REP-2013-003.pdf (accessed on 11 April 2021).
19. Fujii, K.; Grojean, C.; Peskin, M.E.; Barklow, T.; Gao, Y.; Kanemura, S.; Kim, H.; List, J.; Nojiri, M.; Perelstein, M.; et al. Physics Case for the 250 GeV Stage of the International Linear Collider. *arXiv* **2017**, arXiv:1710.07621.
20. Chae, Y.J.; Perelstein, M. Dark Matter Search at a Linear Collider: Effective Operator Approach. *J. High Energy Phys.* **2013**, *1305*, 138. [CrossRef]
21. Martinez, M.; Miquel, R. Multi-parameter fits to the t-tbar threshold observables at a future e^+e^- linear collider. *Eur. Phys. J. C* **2003**, *27*, 49. [CrossRef]
22. Horiguchi, T.; Ishikawa, A.; Suehara, T.; Fujii, K.; Sumino, Y.; Kiyo, Y.; Yamamoto, H. Study of top quark pair production near threshold at the ILC. *arXiv* **2013**, arXiv:1310.0563.
23. Marquard, P.; Smirnov, A.V.; Smirnov, V.A.; Steinhauser, M. Quark mass relations to four-loop order. *Phys. Rev. Lett.* **2015**, *114*, 142002. [CrossRef] [PubMed]
24. Richard, F. Present and future constraints on top EW couplings. *arXiv* **2014**, arXiv:1403.2893.
25. Pavek, M. A Talk Delivered at the International Workshop on Future Linear Colliders LCWS2019, Sendai, Japan. Available online: https://agenda.linearcollider.org/event/8217/contributions/44502/ (accessed on 11 April 2021).